

Ramp-type junction parameter control by Ga doping of $\text{PrBa}_2\text{Cu}_3\text{O}_{7-\delta}$ barriers

M. A. J. Verhoeven,^{a)} G. J. Gerritsma, and H. Rogalla

Department of Applied Physics, University of Twente, P. O. Box 217, 7500 AE Enschede, The Netherlands

A. A. Golubov

Institut für Schicht- und Ionentechnik, Forschungszentrum Jülich GmbH, 52455 Jülich, Germany

(Received 29 March 1996; accepted for publication 28 May 1996)

We analyzed the transport of charge carriers across $\text{PrBa}_2\text{Cu}_{3-x}\text{Ga}_x\text{O}_{7-\delta}$ (PBCGO) barriers as a function of barrier thickness, Ga-doping level, temperature, and bias voltage. It was found that by Ga doping, the normal state resistance (R_n) of the junctions was systematically increased, while the critical current (I_c) remained constant. We argue that pair transport takes place by direct tunneling, whereas the quasiparticles have access to channels formed by one or more localized states inside the barrier. By Ga doping the $I_c R_n$ products were increased, up to 8 mV at 4.2 K for junctions with 8 nm thick $\text{PrBa}_2\text{Cu}_{2.6}\text{Ga}_{0.4}\text{O}_{7-\delta}$ barriers. © 1996 American Institute of Physics.

[S0003-6951(96)03932-0]

To date, all high- T_c weak links show reduced $I_c R_n$ values compared to the expected gap voltage of about 20 mV for $\text{YBa}_2\text{Cu}_3\text{O}_{7-\delta}$ (YBCO).¹⁻⁶ Deutscher *et al.*⁷ argued that highly resistive junction barriers are most feasible for obtaining high $I_c R_n$ values.

For the use of highly resistive barriers, $\text{PrBa}_2\text{Cu}_3\text{O}_{7-\delta}$ (PBCO) is an obvious choice as it is the only pure 123-compound that is not superconducting nor metallic at any temperature.⁸ It was shown however⁹ that the metallic state and also superconductivity can be induced into PBCO by small Ca doping, illustrating how close the material is to the insulator-metal transition. Bulk PBCO is reported to behave like a variable-range hopping (VRH) conductor, caused by the relatively high density of localized states (LS) in the material.¹⁰ The nature of LS is likely to be connected with some kind of structural disorder.¹¹⁻¹³ It has been shown that the resistivity of PBCO can be increased tremendously by substituting copper by gallium into the chain layers.¹⁴ The higher valence of Ga compared to that of Cu then causes a reduction of the density of LS.

In the case of superconductor/insulator/superconductor (SIS) structures, with a high density of LS in the I layer, apart from direct tunneling also indirect (resonant) tunneling via these states *inside* the barrier may take place.¹⁵ Especially at high barrier thickness these resonant contributions may become nonnegligible or even dominant.¹⁶ The total conductivity (G_{tot}) consists of different conduction “channels” in parallel. The direct tunnel process and the one via 1 LS are largely independent of temperature and bias voltage and can be taken together into the linear part of the conductance (G_{lin}), yielding

$$G_{\text{tot}} = G_{\text{lin}} + G_2(T, V) + G_3(T, V) + \dots \quad (1)$$

Glazman and Matveev¹⁷ derived expressions for the conductivity of a channel formed by n LS, where two important limits of activation can be distinguished:

$$G_n(T, V) \propto T^{(n-2/n+1)/e-2\alpha d/n+1} \quad (eV \ll k_B T) \quad (2)$$

$$G_n(T, V) \propto V^{(n-2/n+1)e-2\alpha d/n+1} \quad (eV \gg k_B T)$$

where α^{-1} is the radius of a LS, and k_B is Boltzmann’s constant.

Ramp-type junctions allow for the use of the well-established c -axis high- T_c thin-film technology while allowing the main current to flow in the ab -plane. A more detailed description of the fabrication procedure has been published elsewhere.¹⁸ Starting from a sputtered YBCO/PBCO bilayer, a ramp with an angle of about 20° with respect to the substrate surface is etched using an Ar-ion beam then the photoresist is removed using acetone. The ramp surface is subsequently ion-beam cleaned at low energy to remove damage from the interface.¹⁹ Next, the ramp is covered by a PBCGO barrier layer and a YBCO counterelectrode. Final junction definition, wiring, and metallization are performed by a conventional photolithographic process. The value for the barrier thickness d used, and is the nominal thickness in the direction perpendicular to the substrate surface, as inferred from the calibrated growth rate. We avoid the need to assume which is the actual direction of charge transport through the barrier.

We used both undoped and doped PBCGO ($x = 0, 0.10,$ and 0.40) as barrier layers in ramp-type junctions to study the effect of doping on the electric transport properties of these barriers.

Figure 1 shows a set of current–voltage characteristics (I – V Cs) at different temperatures for a 10 nm thick PBCO barrier. There is little or no excess current and a clear Fraunhofer-like $I_c(B)$ dependence can be observed (see inset). Junctions showing the described features (about 40%), were selected for the presented study. Therefore, this study is based upon measurements performed on 60 chips fabricated within about three years, each containing 5–10 junctions. The on-chip reproducibility was very good with a 10% spread in junction parameters.

We found by atomic-force microscopy (AFM) analysis²⁰ that PBCO barriers of up to 6 nm thickness will have pin-

^{a)}Electronic mail: w.a.m.aarnink@tn.utwente.nl

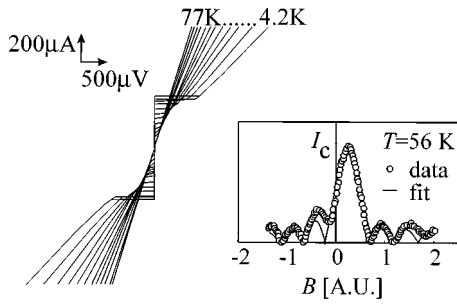


FIG. 1. Typical set of I - V - C 's of a junction with PBCO barrier of $d = 10$ nm at different temperatures. The inset shows the dependence of the critical current at 56 K on the magnetic field applied parallel to the ramp.

holes. This results from the island growth of PBCO and the anisotropy in growth speeds. Therefore, junctions with d up to 6 nm show large excess currents and a very small dependence of I_c on the magnetic field.

Figure 2 shows the linear conductance G_{lin} (formula 1) as a function of the barrier thickness at 4.2 K for PBCGO barriers as determined from the I - V Cs by interpolation. Clearly, the decay parameter can be fitted by a single value ($a = 3.5 \pm 0.5$ nm) up to a PBCO barrier thickness of 50 nm. For 40% Ga doping, the conductivity is reduced by more than one order of magnitude for the whole thickness range studied. Note that the decay parameter is unchanged upon doping.

The constant value of a suggests that only the density of LS in the barrier is changed by Ga doping, and the effective barrier height remained unaffected. The values of the decay parameter a and the radius of a localized state (or: localization length) are equivalent, so: $a = \alpha^{-1}$.¹⁵ From the radius of LS: $\alpha^{-1} = \hbar / (2m_{\text{eff}}U)$ follows (taking for m_{eff} the free electron mass 9×10^{-31} kg) for $\alpha^{-1} = 3.5$ nm: $U = 3$ meV. Although a low band gap value is to be expected for a material which is close to the M-I transition, it seems to be rather low to account for the tunnel data observed up to 10 mV bias and up to some 50 K (Fig. 2).

For thick barriers and high bias voltages, I - V Cs show a positive curvature, indicating an enhancement of the conduc-

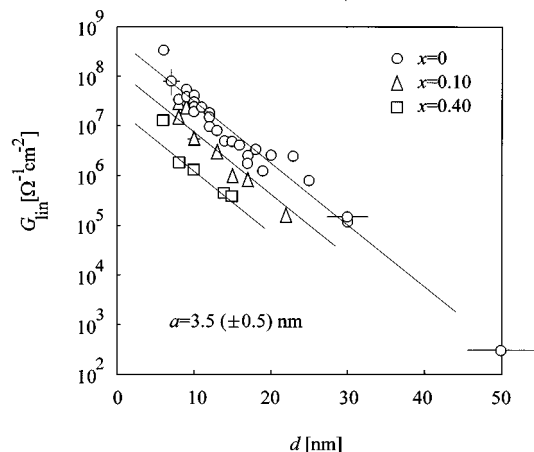


FIG. 2. Low-bias conductance G_{lin} at 4.2 K as a function of the $\text{PrBa}_2\text{Cu}_{3-x}\text{Ga}_x\text{O}_{7-\delta}$ barrier thickness d , for $x=0$; 0.1 and 0.4. The solid lines are guides to the eye.

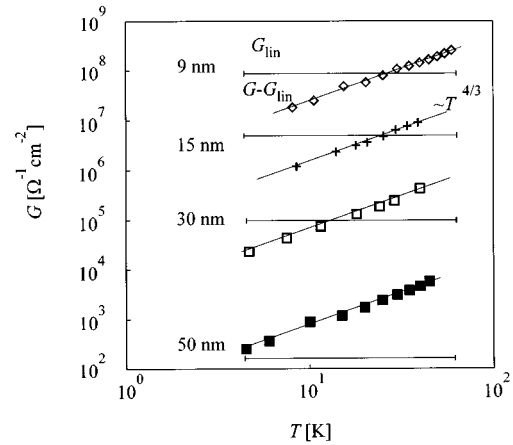


FIG. 3. Plot of the PBCO barrier conductance for different barrier thicknesses as a function of temperature. Horizontal lines depict G_{lin} . Markers show the activated conductance after subtraction of G_{lin} . Solid lines through the markers show the best fit to a $T^{4/3}$ behavior.

tivity. The dependence of this activated conductivity on temperature and bias voltage is shown in Figs. 3 and 4. Because of the limited amount of data available at present on Ga-doped PBCO, this analysis has been restricted to the undoped case. In Fig. 3, the thermal activation is shown by a double-log plot of $G_{\text{tot}} - G_{\text{lin}}$ versus temperature for a range of barrier thickness. Also shown is G_{lin} for each thickness, which is the extrapolation to zero temperature of the linear conductance (horizontal solid lines). The solid lines following the data points are fits to the $T^{4/3}$ dependence, corresponding to indirect passage via 2 LS.

Figure 4 shows a similar analysis for the voltage activation. Although at low voltage the data appear to follow the predicted $V^{4/3}$ reasonably well, for thicker barriers (30 and 50 nm) a clear deviation to higher conductivity is visible. Note however, that the voltage bias activation range is much larger. If equivalent energy scales for temperature and voltage activation are taken ($10^0 - 10^2$ K $\sim 10^{-1} - 10^1$ mV),

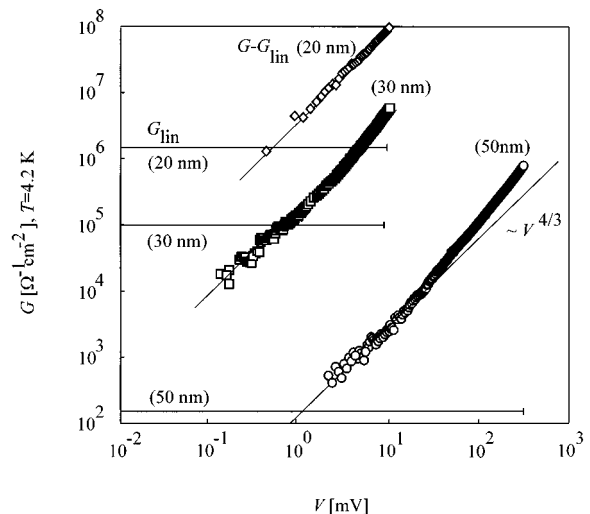


FIG. 4. Plot of the PBCO barrier conductance at 4.2 K as a function of the voltage bias for $d=20$ nm, 30 nm, and 50 nm. Low-bias G_{lin} are depicted, as well as the best fit to a $V^{4/3}$ behavior.

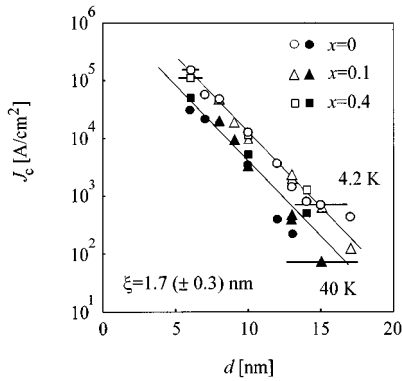


FIG. 5. Critical current density J_c as a function of the $\text{PrBa}_2\text{Cu}_{3-x}\text{Ga}_x\text{O}_{7-\delta}$ barrier thickness d for $x=0$; 0.1 and 0.4 at $T=4.2$ and 40 K. The solid lines are guides to the eye.

the fit to dominant conduction via 2 LS holds quite well in both cases. The deviation shows no evidence for a crossover to the $V^{5/2}$ power law, which is much steeper than the measured voltage dependence. Possibly, the high-voltage branch for the thick barriers already reflects a crossover from the mesoscopic to the macroscopic regime. This would be consistent with the absolute value for the barrier zero-bias resistivity ($\sim 10^3 \Omega \text{ cm}$), as it is already not far from reported values for PBCO thin films at 4.2 K, $\rho_{ab} \approx 10^3 - 10^4 \Omega \text{ cm}$.^{21,22}

Figure 5 shows the exponential decay of the critical current density versus PBCGO barrier thickness d , at 4.2 and 40 K. Note that up to 45 K the decay parameter ($\xi = 1.7 \pm 0.3 \text{ nm}$) remains unchanged. This makes a proximity-effect type of coupling improbable at least up to $0.5T_c$. Second, there is no change in ξ for Ga-doped barriers, having smaller density of LS. This is evidence that the supercurrent is transported by a tunnel process (direct or resonant). Also the supercurrent may be transported via LS.^{17,23} However, Coulomb repulsion might block the resonant passage of pairs, depending on the strength of the pairing interaction and the depth of the LS.^{23,24} Glazman and Matveev²³ showed that the Coulomb repulsion is sufficient to suppress a resonant contribution to the supercurrent, if the resonant line width Γ_0 is very small compared to $k_B T_c$, where $\Gamma_0 = U \exp(-da)$. Since we receive $\Gamma_0 \leq 0.3 \text{ meV}$, this is ob-

viously the case. The observation is that the absolute magnitude of J_c remains constant upon Ga doping, and independent on the density of LS, therefore gives strong evidence that the supercurrent is transported by *direct tunneling*.

The observation that a is about twice the value found for ξ is predicted by formula (2) if the quasiparticle current is transported by 1 LS and the supercurrent by direct tunneling. This is apparently the case here, for low activation.

The systematic increase of barrier resistivity by Ga doping, independent from the junction critical current thus results in an effective enhancement of the $I_c R_n$ products, up to 8 mV at 4.2 K for 8 nm thick $\text{PrBa}_2\text{Cu}_{2.6}\text{Ga}_{0.4}\text{O}_{7-\delta}$.

- ¹M. Gurvitch, J. M. Valles, A. M. Cucolo, R. C. Dynes, J. P. Garno, L. F. Schneemeyer, and J. V. Wasczak, *Phys. Rev. Lett.* **63**, 1008 (1989).
- ²M. Lee and M. R. Beasley, *Appl. Phys. Lett.* **59**, 591 (1991).
- ³R. Dömel, C. Horstmann, M. Siegel, A. I. Braginski, and M. Yu. Kupriyanov, *Appl. Phys. Lett.* **67**, 1775 (1995).
- ⁴K. Char, L. Antognazza, and T. H. Geballe, *Appl. Phys. Lett.* **63**, 2420 (1993).
- ⁵G. Koren and E. Polturak, *Physica C* **230**, 340 (1994).
- ⁶A. W. Kleinsasser and K. A. Delin, *Appl. Phys. Lett.* **66**, 102 (1995).
- ⁷G. Deutscher and R. W. Simon, *J. Appl. Phys.* **69**, 4137 (1991).
- ⁸M. E. López-Morales, D. Ríos-Jara, J. Tagüeña, R. Escudero, S. LaPlaca, A. Bezinge, V. Y. Lee, E. M. Engler, and P. M. Grant, *Phys. Rev. B* **41**, 6655 (1990).
- ⁹D. P. Norton, D. H. Lowndes, B. C. Sales, J. D. Budai, E. C. Jones, and B. C. Chakoumakos, *Phys. Rev. B* **49**, 4182 (1994).
- ¹⁰B. Fisher, G. Koren, J. Genossar, L. Patlagan, and E. L. Gartstein, *Physica C* **176**, 75 (1991).
- ¹¹K. Takenaka, Y. Imanaka, K. Tamasaku, T. Ito, and S. Uchida, *Phys. Rev. B* **46**, 5833 (1992).
- ¹²R. Fehrenbacher and T. M. Rice, *Phys. Rev. Lett.* **70**, 3471 (1993).
- ¹³A. I. Liechtenstein and I. I. Mazin, *Phys. Rev. Lett.* **74**, 1000 (1995).
- ¹⁴Y. Xu and W. Guan, *Physica C* **206**, 59 (1993).
- ¹⁵I. M. Lifshitz and V. Ya. Kirpichenkov, *Sov. Phys. JETP* **50**, 499 (1979).
- ¹⁶Y. Xu, D. Ephron, and M. R. Beasley, *Phys. Rev. B* **52**, 2843 (1995).
- ¹⁷L. I. Glazman and K. A. Matveev, *Sov. Phys. JETP* **67**, 1276 (1988).
- ¹⁸J. Gao, W. A. M. Aarnink, G. J. Gerritsma, D. Veldhuis, and H. Rogalla, *IEEE Trans. Magn.* **27**, 3062 (1991).
- ¹⁹M. A. J. Verhoeven, G. J. Gerritsma, and H. Rogalla, *Proceedings of the Eucas '95 Conference, Edinburgh, 1995*, p. 1395.
- ²⁰M. A. J. Verhoeven, R. Moerman, M. E. Bijlsma, A. J. H. M. Rijnders, D. H. A. Blank, G. J. Gerritsma, and H. Rogalla, *Appl. Phys. Lett.* **68**, 1276 (1996).
- ²¹U. Kabasawa, Y. Tarutani, M. Okamoto, T. Fukazawa, A. Tsukamoto, M. Hiratani, and K. Takagi, *Phys. Rev. Lett.* **70**, 1700 (1993).
- ²²G. K. van Ancum, M. A. J. Verhoeven, D. H. A. Blank, and H. Rogalla, *Phys. Rev. B* **52**, 5598 (1995).
- ²³L. I. Glazman and K. A. Matveev, *JETP Lett.* **49**, 659 (1989).
- ²⁴I. A. Devyatov and M. Yu. Kupriyanov, *JETP Lett.* **59**, 200 (1994).